Canadian Conference - Pacific Conference on Earthquake Engineering 2023

Vancouver, British Columbia

June 25th – June 30th, 2023

Investigating the Impacts of Building Importance Level and Ductile Design on the Performance of Base-Isolated Buildings in New Zealand

Claire Dong[1], Timothy J. Sullivan[2]

[1]PhD Student, Department of Civil Engineering, University of Canterbury, Christchurch, New Zealand
[2]Professor, Department of Civil Engineering, University of Canterbury, Christchurch, New Zealand
[1]claire.dong@pg.canterbury.ac.nz (Corresponding Author)

ABSTRACT

Preliminary seismic isolation design guidelines were recently released in New Zealand to provide both guidance for the design of base-isolated buildings and consistency in their performance. Seismic design in NZ requires selection of an Importance Level (IL1 – IL4) and the guidelines permit the use of strength reduction factors greater than one (i.e ductility greater than one). This study investigates the impacts of building importance level and superstructure ductility on isolated building performance in terms of structural response and collapse. Five 4-story case study buildings were designed following the NZ seismic isolation guidelines and ASCE/SEI 7-22 for a site in Wellington, NZ. Various importance levels and strength reduction factors were assigned. The building performance was assessed using a multiple-stripe Non-Linear Time-History Analysis (NLTHA) approach, executed in OpenSees with 20 pairs of ground motions at nine different intensity levels. The study found that an IL4 building required a higher characteristic strength and post-yield stiffness, hence a higher effective stiffness compared to an IL2 building, which lead to an increase in Peak Floor Acceleration (PFA) and Peak Story Drift (PSD). The PSD was sensitive to the design ductility adopted. Allowing a strength reduction factor of two in the IL4 building did not reduce the PFA compared to the same IL4 building without strength reduction, but it increased the PSD demand by between 200 – 600%. This suggests that an IL4 building with higher ductility may suffer more damage compared to an IL2 building because of its higher PFA and PSD demand and thus it is recommended that the design ductility values permitted for IL4 buildings be reconsidered. The collapse is defined as the attainment of the isolator displacement capacity or wall deformation capacity. The IL2 building had the highest annual rate of collapse, which was 1.84×10^{-4}. The failure was generally governed by isolator failure except when higher ductility was adopted where the wall failure was more likely to govern.

Keywords: Base isolation, Peak floor acceleration, Peak story drift, Collapse fragility

INTRODUCTION

Base isolation is an established strategy to achieve excellent seismic performance of buildings [1-3]. Typically, a base-isolated building consists of a superstructure, isolation plane (including isolators and stability structure), foundation, and rattle space. For a properly designed base isolation system, the acceleration demand in the superstructure is limited and the majority of the displacement demand is expected to concentrate in the isolation plane, which provides the system with a long effective period. The isolators are also designed to dissipate seismic energy or can be paired with damping devices. The damage or loss of a base-isolated building is therefore expected to be lower than traditionally designed buildings. The design process for base-isolated buildings is outlined in some design codes, such as ASCE/SEI 7-22 [4] in the United States and Eurocode 8 [5] in Europe. In New Zealand, base isolation is currently considered an alternative solution due to the lack of acceptable solutions or verification methods cited in the NZ building code. The New Zealand Society for Earthquake Engineering (NZSEE) prepared a preliminary version of the "*Guideline for the Design of Seismic Isolation Systems for Buildings*" [6] for trial use and industry comment. The guideline is relatively new and references the US and European codes. This study investigates the impacts of some of the design choices such as the importance level and strength reduction factor (i.e. the design ductility) on base-isolated building performance.

METHODOLOGY

To investigate the impact of design choices on building performance, a set of case study buildings are designed in line with the base isolation design guidelines in NZSEE/MBIE [6] and ASCE/SEI [4]. The building performance is assessed using a multiple-stripe Non-Linear Time-History Analysis (NLTHA) approach, executed in OpenSees with 20 pairs of ground motions at nine different intensity levels.

Case study buildings

Previous research reported in [7] developed a design solution for a 4-storey RC wall building shown in Figure 1a. The isolated versions of the same building were then designed [8] to permit building performance to be compared. The configuration of the superstructure in this study remains the same, with the lateral resisting system consisting of six short RC walls in the X direction and two long RC walls in the Y direction, as shown in Figure 1a. The total footprint is 24 m by 40 m, the first story is 4.5 m and the stories above are 3.6 m. The isolation plane layout is presented in Figure 1b. It consists of 14 Lead Rubber Bearings (LRBs) and 8 Flat Sliders (FSs). The isolators are connected through grillage beams.

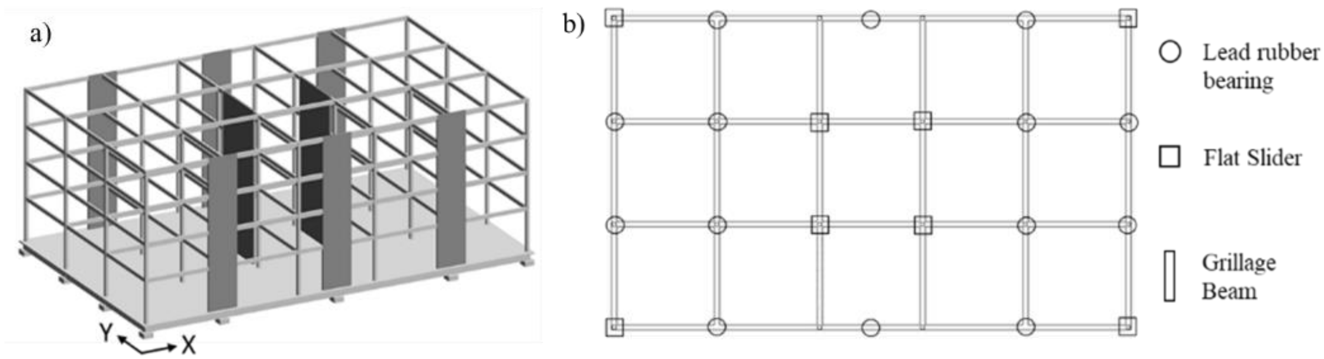

Figure 1: Case study building: a) 3D view and b) isolation plane view (figures from [8])

Design criteria

The New Zealand seismic design standards, NZS1170.5:2004 [9] provides means of estimating the seismic design coefficients in New Zealand. The elastic site hazard spectrum for horizontal loading is a function of spectral shape factor ($C_h(T)$) that accounts for site subsoil class and building period; hazard factor (Z); near-fault factor (N(T, D)); and return period factor (R) that considers the design return period or an annual probability of exceeding a given intensity [9]. A damping reduction factor (η) may be applied to the elastic site hazard spectrum depending on the characteristics of the isolation plane design. In summary, the site hazard spectrum can be computed using Eq. (1).

$$C(T) = C_h(T) \cdot Z \cdot N(T, D) \cdot R \cdot \eta \tag{1}$$

NZS1170.5:2004 [9] requires the building to be checked for a Serviceability Limit State (SLS) and the Ultimate Limit State (ULS). The return periods of the shaking intensity at these limit states are assigned based on the Importance Level (IL) of the building. For example, a hospital will be an IL4 design and the return period of the intensity at the ULS is 2500 years. Whereas a medium-density residential building will typically be designed as IL2 with a corresponding return period of 500 years at the ULS. The NZSEE/MBIE base isolation design guidelines [6] recommend design checks for two additional limit states: a Damage Control Limit State (DCLS) and Collapse Avoidance Limit State (CALS). The typical performance and design checks at these limit states include avoidance of superstructure yielding at the SLS; superstructure story drift limits at the DCLS (typically 0.5%, depending on designer's choice); superstructure strength, story drift (2.5%), and isolator stability limits at the ULS; and isolator displacement and rattle space checks at the CALS. In contrast, the ASCE/SEI 7-22 does not have importance level factors assigned to base-isolated buildings. Unlike the limit-state design approach in New Zealand, both the isolation plane and superstructure are designed at the Risk-Targeted Maximum Considered Earthquake (MCE_R) intensity level, which has a probability of exceedance of 2% in 50 years, equivalent to a return period of 2475 years.

Design procedure and results

Five different design solutions are developed for a 4-storey case study building; three designs follow the NZ isolation guidelines, including an IL2 building and two IL4 buildings. The other two building designs follow the ASCE/SEI 7-22 code, with no consideration of building importance and different design limit states. These case study buildings are further divided by the superstructure design ductility which will be discussed more in detail. The buildings are assumed to be located in Wellington, New Zealand and have a V_{S30} of 450 m/s, which can be classified as subsoil class C. The seismic design parameters are reported in Table 1.

Table 1: Seismic design parameters that are used to construct the hazard spectrum.

Seismic design parameters	**NZ guideline (IL2)**	**NZ guideline (IL4)**	**ASCE/SEI 7-22**
Hazard factor, Z	0.4	0.4	0.4
Return period factor, $R_{SLS1/SLS2}$	0.25	1	
R_{DCLS}	0.75	-	MCE_R, 1.8
R_{ULS}	1	1.8	
R_{CALS}	1.5	2.34	
Spectral shape factor, $C_h(T)$*	0.53	0.56	0.50
Near-fault factor, N(T, D)*	1.24	1.20	1.28
Damping reduction factor, η*	0.483	0.493	0.581

*Note: these parameters depend on the period of the system and values based on the nominal effective period at the ULS are reported.

Following the design process recommended by the guidelines, the building weight is estimated based on the preliminary design and may be refined later. Including the base slab above the isolators and four stories, the total seismic weight of the case study building is 34566 kN. The isolation plane is designed using the capacity-spectrum method [10] assuming the superstructure is a rigid block, and the system behaves as a Single Degree of Freedom (SDOF) system. The stability and uplifting of the isolators are checked at the ULS, whereas the isolator displacement and rattle space are checked at the CALS. The design results of the isolation plane are reported in Table 2, including the characteristic strength (Q_d), post-yield stiffness (K_d), the ratio of post-yield stiffness to initial stiffness (α), the total thickness of the rubber layer (t_e), the maximum displacement demand at the CALS (D_M) using lower bound isolator properties, and the corresponding effective period of the isolation system (T_{eff}).

Table 2: Case study building solation system design results

Isolator Design Parameters	**NZ guidelines (IL2)**	**NZ guidelines (IL4)**	**ASCE/SEI 7-22**
System characteristic strength, Q_d	2037 kN	3717 kN	2793 kN
System post-yield stiffness, K_d	12.1 kN/mm	13.9 kN/mm	13.8 kN/mm
System stiffness ratio, α (K_d / K_i)	0.0578	0.0667	0.629
Total thickness of rubber, t_e	200 mm	250 mm	200 mm
Maximum isolator displacement demand, D_M	576 mm	709 mm	560 mm
Effective period at D_M, $T_{eff,\ Dm}$	3.28 s	2.97 s	2.99 s

In this study the rattle space is assumed to be sufficient around the buildings and the isolation plane designs are generally governed by the isolator displacement capacity. The difference in the isolation plane designs is a result of the difference in R_{CALS} factors listed in Table 1. The isolation system tends to require a higher characteristic strength, post-yield stiffness, and displacement capacity as R_{CALS} increases.

The design process of the superstructure of the isolated building is similar to that of a traditional building. The design base shear is distributed to the superstructure using methods such as Equivalent Static Analysis (ESA) or Modal Response Spectrum (MRS) method, the building may need to be verified with NLTHA depending on the building IL. According to the isolation design guidelines [6], the IL2 case study building may be classified as Type 1 - Simple, which permits the use of ESA. The strength reduction factor of one ($k_\mu = 1$) is required at the ULS, meaning the superstructure is designed to respond elastically. The IL4 case study buildings are classified as Type 3 – Ductile, which also requires the design to be verified using NLTHA. A strength reduction factor of up to two ($k_\mu \leq 2$) is allowed for Type 3 buildings at the ULS, meaning the superstructure is allowed to develop some ductility. Similarly, a strength reduction factor (the ρ factor) of up to two is permitted in ASCE7-22. To investigate the effects of allowing the superstructure to develop ductility, the IL4 buildings and ASCE buildings are designed using k_μ of one and two. The design results are presented in Table 3. The superstructure designs are all governed by strength checks. Interestingly, the superstructure design results of the elastically designed buildings end up being similar and the superstructures designed using strength reduction factors both have similar designs.

Numerical models

The previous section described the case study building design results which are based on the upper bound, lower bound, and nominal isolator properties, and characteristic design properties for the superstructure. However, to assess the performance, probable design properties are assigned in the numerical models described in this section. The 3D numerical models are developed in OpenSees [11]. The Lead Rubber Bearings (LRBs) are modeled using bilinear hysteretic models and the Flat Sliders (FSs) are modeled using Coulomb friction models. The isolators are connected by the grillage beams that have a large in-plane stiffness; hence the isolation plane can be considered a rigid diaphragm. The RC walls are modelled as elastic cantilevers with cracked section stiffness estimated based on [12]. At the bottom of each RC wall, a plastic hinge is inserted to enable plastic deformations to occur. The overall behavior of the wall and hinge follows a Takeda hysteretic model [13]. The gravity frames are modelled as truss elements that only provide gravity support and aim to facilitate P-Delta actions to be introduced. Rigid diaphragm constraints are applied to the RC walls and gravity frames at each floor. Seismic mass and gravity loads are assigned to walls and frames based on their tributary area. A Rayleigh damping model is applied with 3% damping at the first and fourth modes.

Table 3: Case study building superstructure design results

Superstructure Design Parameters	**NZ (IL2)**	**NZ (IL4)**	**NZ (IL4)**	**ASCE**	**ASCE**
Strength reduction factor, k_μ	1	1	2	1	2
Superstructure base shear, $S_{a, ULS}$	0.19 g	0.36 g	0.36 g	0.35 g	0.35 g
Wall dimension (per wall)	3 × 0.4 m	4 × 0.4 m	3 × 0.4 m	4 × 0.4 m	3 × 0.4 m
Nominal flexural strength, $M_{n, x}$	10270 kNm	20308 kNm	10270 kNm	20308 kNm	10270 kNm
Reinforcement ratio, $\rho_{b, x}$	1.15%	1.35%	1.15%	1.35%	1.15%
Axial load ratio	2.2%	1.9%	2.2%	1.9%	2.2%
Fixed-base period $T_{fixed, x}$*	0.56 s	0.37 s	0.56 s	0.37 s	0.56 s
Wall dimension (per wall)	6 × 0.4m	7 × 0.4 m	6 × 0.4 m	7 × 0.4 m	6 × 0.4 m
Nominal flexural strength, $M_{n, y}$	29989 kNm	58884 kNm	29989 kNm	56166 kNm	29989 kNm
Reinforcement ratio, $\rho_{b, y}$	0.79%	1.30%	0.79%	1.23%	1.30%
Axial load ratio	2.2%	2.0%	2.2%	2.0%	2.2%
Fixed-base period $T_{fixed, y}$*	0.36 s	0.29 s	0.36 s	0.29 s	0.36 s

* T_{fixed} of the superstructure is estimated using the Rayleigh method and the displacement profile is estimated using the effective section properties as per NZS 3101:2006 [14].

Non-linear time history analysis

Numerical models of the buildings were developed and subject to multiple-stripe (MS) NLTHA to assess the performance of the case study buildings. The numerical models were loaded bi-directionally using the selected ground motions [15]. Vertical excitation is not included in the scope of this study and is not expected to influence the behavior significantly. The ground motions were selected and scaled for the case study building site at SA(2.0s) using the generalized conditioning intensity measure approach [16], considering the 2010 New Zealand National Seismic Hazard Model [17]. The ground motion set used for MSA consists of 180 pairs of hazard-consistent ground motions across nine intensity levels, with 20 pairs for each intensity. The design hazard curve from NZS 1170.5 and the ground motion hazard curve are plotted in Figure 2a. An example of the design spectral acceleration and pseudo-spectral acceleration of the ground motions at intensity level six (corresponding to a 2500-yr return period) are plotted in Figure 2b.

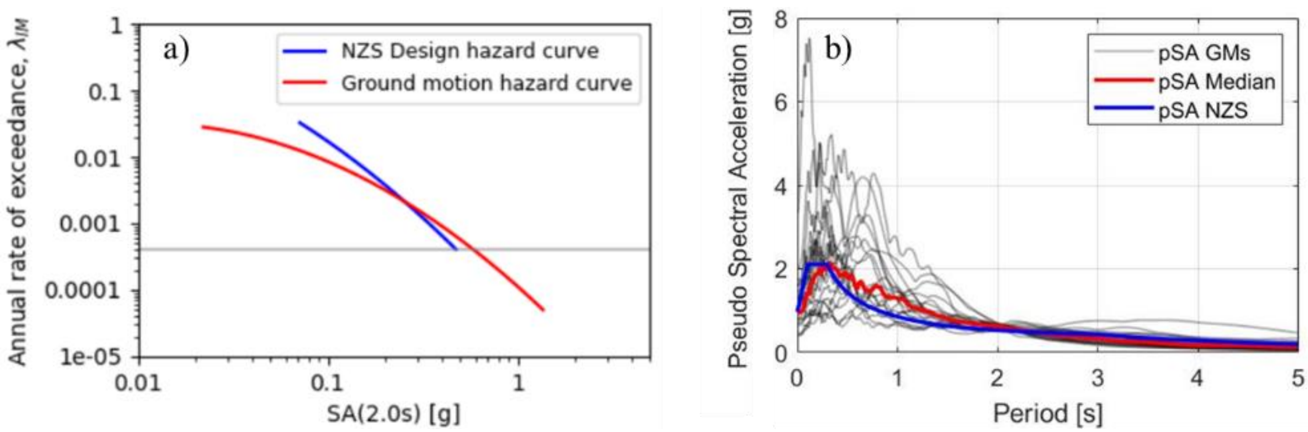

Figure 2: Comparison of a) design hazard curve and ground motion hazard curve, and b) design spectral acceleration and pseudo-spectral acceleration of the ground motions corresponding to a 2500-yr return period.

STRUCTURAL RESPONSE

The structural response under bi-directional loading is recorded during the NLTHA, including the lead rubber bearing displacement, base shear, floor acceleration, and story drift. The base shear is normalized by the total building weight and reported as a coefficient. The maximum base shear coefficient and LRB displacement are evaluated considering the combined demands from orthogonal directions. The median values at each intensity are plotted in Figure 3a and 3b, respectively. Comparing the base shear coefficient of the three case study buildings, it is observed that the IL4 buildings experience slightly larger base shear than the ASCE buildings, and the IL2 building experiences relatively lower base shear. Figure 3b compares the maximum LRB displacement of the case study buildings. It appears that the LRB displacement demand is larger for the IL2 building, followed by the ASCE buildings, and the IL4 buildings. The difference in base shear and displacement demand can be explained by the difference in effective stiffness of the isolation system which is a combination of characteristic strength (Q_d) and post-yield stiffness (K_d). However, for intensities that are higher than around 0.8g, the stiffness differences do not explain the differences, which are instead likely to be due to yielding of the superstructure at higher intensity levels.

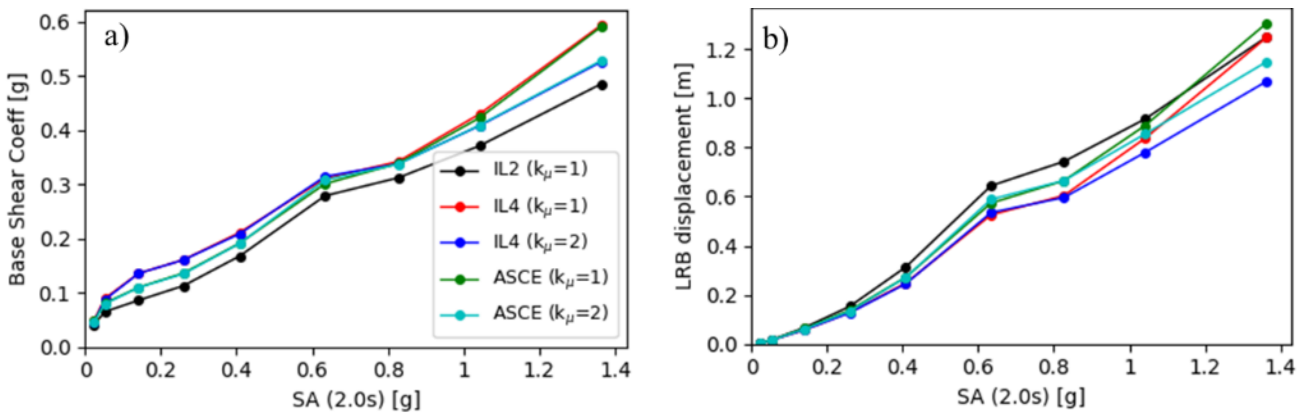

Figure 3: Peak isolation system demand: a) the maximum base shear normalised by building weight, and b) the maximum Lead Rubber Bearing (LRB) dispalcement demand.

The median values of Peak Floor Acceleration (PFA) and Peak Story Drift (PSD) among all stories and both directions are plotted against the intensities in Figure 4a and 4b, respectively. The PFA demands are the highest for the two IL4 buildings, followed by the ASCE buildings and the IL2 building. This is similar to what was observed for the isolation system base shear. The numerical study by [18] made similar observations where the superstructure response tends to increase with the increase of the yield strength of the isolation system. The PSD demands are expected to be higher for superstructures that have less stiffness (recall that the stiffness of the RC walls is set to be proportional to their strength [12]). It is also expected that once the wall yields, the difference in the PSD demands will be even more significant. However, it is interesting to see that allowing ductility design, and subsequently a more flexible superstructure, did not reduce the PFA; the reduction only takes place once the walls yield at higher intensities. The study by [19] observed similar results noting that a base-isolated braced frame building that had a higher ductility reduced the PFA by just 20% but increased the PSD by up to 75%.

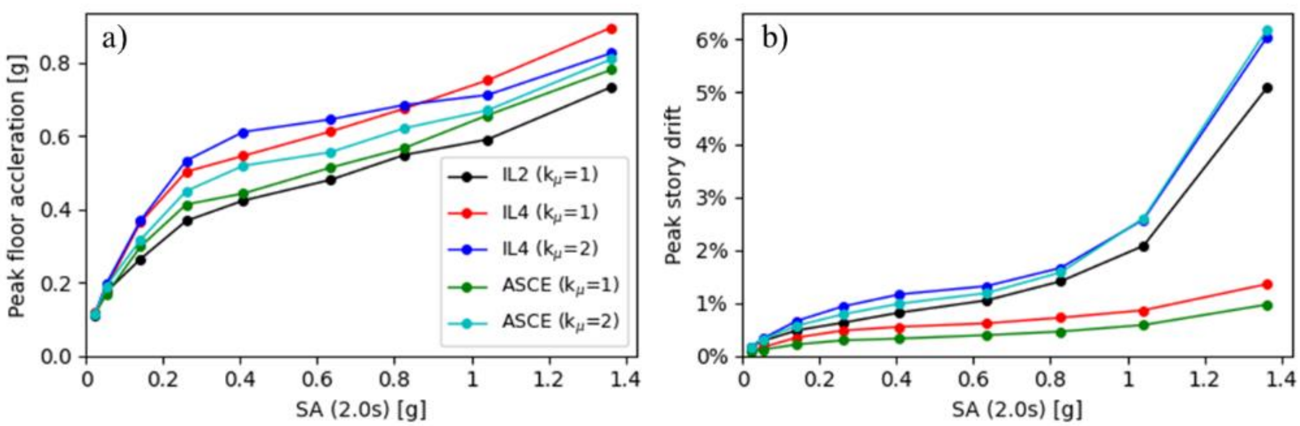

Figure 4: Peak superstructure demand: a) peak floor acceleration, and b) peak story drift.

STRUCTURAL COLLAPSE

To investigate the structural performance in terms of collapse, a collapse fragility function is developed for each case study building and the annual rate of collapse (λ_c) is computed using Eq. (2).

$$\lambda_c = \int_{IM_i}^{IM_f} P(collpase|IM = x) \cdot |d\lambda_{IM}(x)| \tag{2}$$

The term $P(collpase|IM = x)$ is the fragility function of the structure which describes the probability of collapse at an intensity x, $|d\lambda_{IM}(x)|$ is the annual rate of occurrence of the specific intensity x. The integration domain $IM_i \leq x \leq IM_f$ is defined in a way that the contribution to the annual rate of collapse from outside this domain is negligible because it either has a very small probability of collapse or a very small rate of occurrence. The collapse fragility function is developed using the Maximum Likelihood method, technical details are explained in [20]. Firstly, based on the MS NLTHA results, the fraction of the ground motions at each intensity measure level that causes collapse is identified. Then a median (θ) and dispersion (β_{rtr}) is defined such that the fragility function has the highest probability to produce the observed collapse fraction at each intensity level. Note that β_{rtr} is the record-to-record variability. The fragility function is then modified using the double-lognormal fragility model to include modelling uncertainty (β_m) [21], [22]. The total dispersion becomes $\beta_c = \sqrt{\beta_{rtr}^2 + \beta_m^2}$. A β_m of 0.354 is used in this study based on FEMA P-58 [23] and assuming the building has an average construction and numerical model quality.

Collapse definition

The building collapse is triggered when either of the following criteria is exceeded: (i) the drift demand of the superstructure exceeds the RC wall drift capacity; or (ii) the shear strain of the LRB exceeds 500%. The equation proposed by [24] is used to estimate the RC wall drift capacity, which is a function of the wall dimensions, neutral axis depth, shear stress, and concrete compressive strength. The drift capacities for the short walls in the X-direction of the five case study buildings are around 3.5% - 3.7%. For the longer walls in the Y-direction, the drift capacities are around 2.7% - 3.2%. The experimental tests used to derive the drift capacity equation generally consisted of a single wall specimen with a point load at the top [24]. As the case study building has four stories, it would be conservative to compare the peak story drift (occuring at roof level) with the wall drift capacity (expected to develop at ground storey) directly. Therefore, the drift demand of the superstructure is estimated by converting the multistory building into an equivalent SDOF system [12]. The shear strain of the LRB is defined as the horizontal displacement normalized by the total thickness of the rubber layers. The experimental tests on LRBs have shown that rubber hardening is unlikely to occur until at least 400% shear strain [25] [26] [27]. Based on the test results and information provided in the LRB product catalog, a maximum shear strain capacity of 500% is adopted in this study.

Collapse fragility and the annual rate of collapse

The global collapse fragility curves of the three case study buildings are plotted in Figure 5a. The median values, dispersions of these fragility curves and their annual rate of collapse are reported in Table 4. The IL2 building has the highest annual rate of collapse (1.84×10^{-4}), followed by the ASCE building with a $k_\mu = 2$ (1.36×10^{-4}), the ASCE building with a $k_\mu = 1$ (1.13×10^{-4}), the IL4 building with a $k_\mu = 2$ (1.00×10^{-4}), and the IL4 building with a $k_\mu = 1$ (0.90×10^{-4}). To better understand which failure mechanism is more likely to govern, the collapse fragilities of the LRBs and RC walls are plotted separately in Figures 5b – 5f. The fragility function parameters and the annual rate of collapse are reported in Table 5. It appears that the LRB failure tends to be the failure mechanism for the buildings with a $k_\mu = 1$. Whereas the use of a strength reduction factor ($k_\mu = 2$) in the RC wall seems to shift the wall failure fragility curve to the left and results in the superstructure failing before the isolators. This outcome is arguably not desirable as it implies that the isolation devices have not been fully utilized.

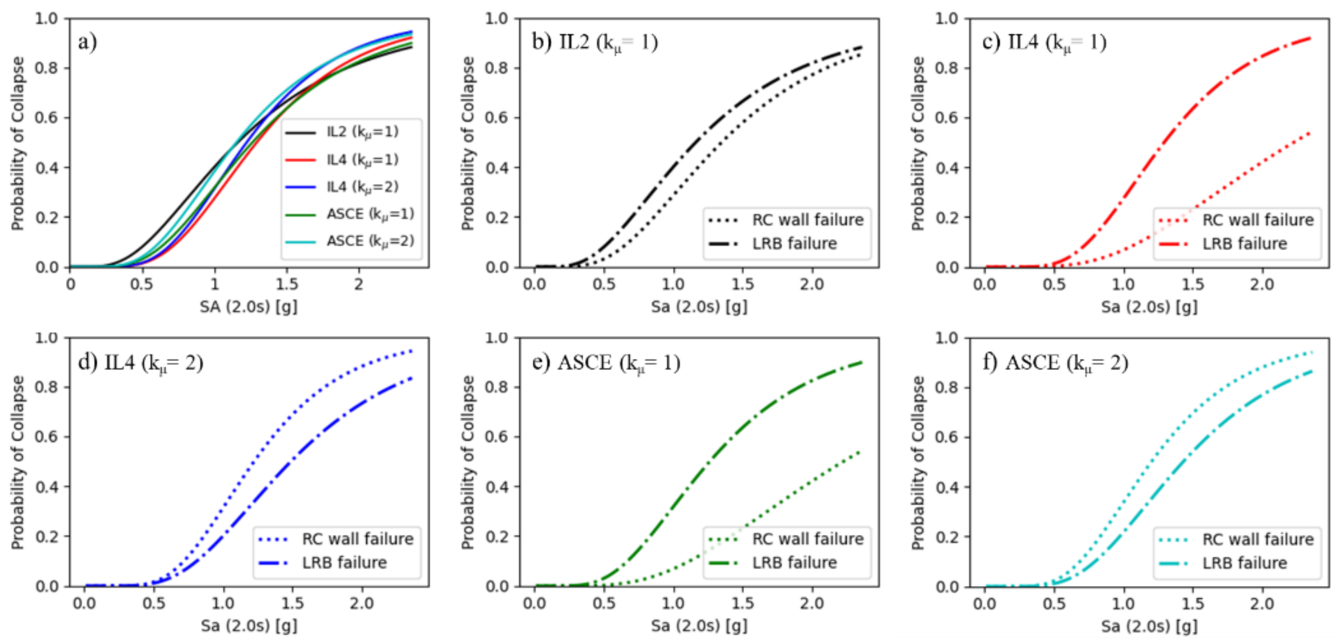

Figure 5: Collpase fragility curves of the three isolated case study buildings: a) global collapse fragility, and b-f) RC wall failure fragilities and Lead Rubbber Bearing (LRB) failure fragilities plotted seperately for each of the case study buildings.

Table 4: Fragility curves parameters and annual rate of collapse.

	NZ guideline (IL2, $k_\mu = 1$)	**NZ guideline (IL4, $k_\mu = 1$)**	**NZ guideline (IL4, $k_\mu = 2$)**	**ASCE7-22 ($k_\mu = 1$)**	**ASCE7-22 ($k_\mu = 2$)**
Median, θ_c	1.16 g	1.30 g	1.23 g	1.27 g	1.15 g
Dispersion, β_c	0.48	0.43	0.42	0.49	0.48
Annual rate of collapse, λ_c	1.84×10^{-4}	0.90×10^{-4}	1.00×10^{-4}	1.13×10^{-4}	1.36×10^{-4}

Table 5: Collapse fragility curves parameters of the RC wall and Lead Rubber Bearings (LRBs)

	NZ guideline (IL2, $k_\mu = 1$)	**NZ guideline (IL4, $k_\mu = 1$)**	**NZ guideline (IL4, $k_\mu = 2$)**	**ASCE7-22 ($k_\mu = 1$)**	**ASCE7-22 ($k_\mu = 2$)**
Median, $\theta_{c,wall}$	1.35 g	2.14 g	1.23 g	2.23 g	1.21 g
Dispersion, $\beta_{c,wall}$	0.40	0.54	0.42	0.54	0.48
Annual rate of collapse, λ_c	1.07×10^{-4}	0.27×10^{-4}	1.00×10^{-4}	0.27×10^{-4}	1.22×10^{-4}
Median, $\theta_{c,LRB}$	1.16 g	1.30 g	1.49 g	1.27 g	1.24 g
Dispersion, $\beta_{c,LRB}$	0.48	0.43	0.47	0.49	0.49
Annual rate of collapse, λ_c	1.84×10^{-4}	0.90×10^{-4}	0.69×10^{-4}	1.13×10^{-4}	1.18×10^{-4}

CONCLUSIONS

This study investigated the impacts of building importance factors and superstructure ductility (controlled via the strength reduction factor) on base-isolated building performance. The performance is expressed in terms of isolator displacement, peak floor acceleration, peak story drift, and collapse fragility. Five different designs were developed for a 4-storey case-study building in Wellington, New Zealand, and NLTHA were performed in OpenSees. Three of the design solutions followed the recommendations provided in the NZSEE/MBIE base isolation design guidelines and two followed the ASCE/SEI 7-22 requirements. For the NZ designs, one adopts a classification of IL2, two buildings adopt a classification of IL4. For the ASCE designs, buildings do not have importance levels. According to the guidelines, the IL2 building is required to respond elastically at the Ultimate Limit State (ULS) intensity. Whereas a strength reduction factor (k_μ) of up to two is permitted for the IL4 buildings and the ASCE buildings to allow non-linear ductile response. The design results and multiple-stripe NLTHA results show that:

- The IL4 buildings required the isolation system to have a larger capacity than the IL2 building, including a higher characteristic strength, post-yield stiffness, and isolator displacement capacity. This increased the peak floor acceleration (PFA) and reduced the peak story drift (PSD) when $k_\mu = 1$ was used. The isolator displacement demand was also reduced.
- Permitting the superstructure to develop ductility in isolated buildings did not reduce the PFA demand. Furthermore, it significantly increased the PSD demand by a factor of two to six times. The comparison showed that the IL4 building with a $k_\mu = 2$ had higher PFA and similar PSD demands to the IL2 building. From a damage and loss point of view, this could mean that the IL4 building with higher ductility is likely to suffer more damage at low to medium intensity earthquakes that are more frequent.
- The IL2 building has the highest annual rate of collapse (1.84×10^{-4}), followed by the ASCE building with a $k_\mu = 2$ (1.36×10^{-4}), ASCE building with a $k_\mu = 1$ (1.13×10^{-4}), IL4 building with a $k_\mu = 2$ (1.00×10^{-4}), and the IL4 building with a $k_\mu = 1$ (0.90×10^{-4}). The collapses of the IL4 and ASCE buildings with $k_\mu = 2$ were governed by the RC wall failure. Whereas the collapse for the rest of the buildings is governed by LRB failure.

Overall, it was found that increasing the importance level of base-isolated building from IL2 to IL4 resulted in better structural performance and a lower annual rate of collapse. However, when a strength reduction factor of two was permitted for the IL4 building, it performed worse than the IL2 building in terms of PFA and PSD, which suggested more damage and hence repair costs would be observed in the superstructure, especially to the drift-sensitive components. This finding is not considered desirable and if future research for other case-study buildings confirms this trend, revisions to the NZ base-isolation guidelines would be recommended.

ACKNOWLEDGMENTS

This project was also partially supported by the Resilience to Nature's Challenges project-built environment theme. This project was also partially supported by QuakeCoRE, a New Zealand Tertiary Education Commission-funded Centre. This is QuakeCoRE publication number 0861.

REFERENCES

[1] Christopoulos, C., and Filiatrault, A. (2006). *Principles of Passive Supplemental Damping and Seismic Isolation*. 1st Edition. ISBN-10: 8873580378. IUSS Press.

[2] Skinner, R.I., Robinson, W.H., and McVerry, G.H. (1993). *An introduction to seismic isolation*. John Wiley & Sons, Chichester, U.K , and New York, 1993, 354pp. https://doi.org/10.1111/j.1475-1305.1993.tb00842.x

[3] Stanton, J., and Roeder, C., (1991). "Advantages and Limitations of Seismic Isolation". *Earthquake Spectra*, **7**(2), 301–324. http://dx.doi.org/10.1193/1.1585630

[4] ASCE/SEI. (2017). *Minimum Design Loads and Associated Criteria for Buildings and Other Structures: ASCE/SEI 7-22*. American Society of Civil Engineers. https://doi.org/10.1061/9780784415788

[5] Europena Committee for Standarization. (2004). *Eurocode 8: Design of structures for earthquake resistance – Part 1: General rules, seismic actions and rules for buildings*. London: British Standards Institution.

[6] NZSEE/MBIE. (2019). *Guideline for the Design of Seismic Isolation Systems for Buildings*. New Zealand Society of Earthquake Engineering. https://www.nzsee.org.nz/wp-content/uploads/2019/06/2825-Seismic-Isolation-Guidelines-Digital.pdf

[7] John, L., Williamson, M.B., and Sullivan, T.J. (2022). "Investigating the Impact of Design Criteria on the Expected Seismic Losses of Multi-Storey Office Buildings". *Bulletin of the New Zealand Society for Earthquake Engineering*, **56**(1).

[8] Dong, C., Sullivan, T.J., and Pettinga, D. (under review) "Investigating the impacts of design ductility values and importance levels on the performance of base-isolated buildings" *Bulletin of the New Zealand Society for Earthquake Engineering*, **xx**(x).

[9] Standards New Zealand. (2016). *NZS 1170.5:2004 Structural Design Actions - Part 5: Earthquake Actions – New Zealand*. Standards New Zealand. https://www.standards.govt.nz/shop/nzs-1170-52004/

[10] Freeman, S.A. (1978). "Prediction of Response of Concrete Buildings to Severe Earthquake Motion" in "*Proceedings of Douglas McHenry International Symposium on Concrete and Concrete Structures*", Publication SP-55, American Concrete Institute, Detroit, Michigan, U.S.A.

[11] McKenna, F., (2011). "OpenSees: A Framework for Earthquake Engineering Simulation. *Computing in Science & Engineering"*, **13**(4), 58–66. https://doi.org/10.1109/MCSE.2011.66

[12] Priestley, M.J.N., Calvi, G.M., & Kowalsky, M.J. (2007). *Displacement-based Seismic Design of Structures*. IUSS Press. https://doi.org/10.1016/S0141-0296(98)00093-5

[13] Otani, S. (1981). "Hysteretic models for reinforced concrete for earthquake analysis". *Facility of Engineering*, **XXXVI**(2): 125-156.

[14] Standards New Zealand (2006). *NZS 3101:2006. Concrete Structures Standard*. Standards New Zealand, Wellington, 756pp.

[15] Yeow, T.Z., Orumiyehei, A., Sullivan, T.J., MacRae, G.A., Clifton, G.C., & Elwood, K.J. (2018). "Seismic performance of steel friction connections considering direct-repair costs". *Bulletin of Earthquake Engineering*, **16**(12): 5963–5993. https://doi.org/10.1007/s10518-018-0421-x

[16] Bradley, B.A. (2010). "A generalized conditional intensity measure approach and holistic ground-motion selection". *Earthquake Engineering and Structural Dynamics*, **39**:1321–1342. https://doi.org/10.1002/eqe.995

[17] Stirling M, McVerry G, Gerstenberger M, Litchfield N, Van Dissen R, Berryman K, Barnes P, Wallace L, Villamor P, Langridge R, Lamarche G, Nodder S, Reyners M, Bradley B, Rhoades D, Smith W, Nicol A, Pettinga J, Clark K, & Jacobs K (2012). "National Seismic Hazard Model for New Zealand: 2010 Update". *Bulletin of the Seismological Society of America*, **102**(4):1514-1542. https://doi.org/10.1785/0120110170

[18] Mavronicola, E. and Komodromos, P. (2014). "On the response of base-isolated buildings using bilinear models for LRBs subjected to pulse-like ground motions: Sharp vs. smooth behaviour" *Earthquakes and Structures*, **7**(6): 1223.

[19] Jalali, Y., Amiri, G.G., and Shakouri, A. (2021). "Comparative response assessment of base-isolated braced-frame buildings considering effects of ductility design" *Journal of Building Engineering*, **43**: p. 103110, Nov. 2021.

[20] Baker, J.W. (2015). "Efficient analytical fragility function fitting using dynamic structural analysis" *Earthquake Spectra*, **31**(1): 579–599.

[21] Kennedy, R.P., Cornell, C.A., Campbell, R.D., Kaplan, S., and Perla, H.F. (1980). "Probabilistic seismic safety study of an existing nuclear power plant" *Nucl. Eng. Des*., **59**(2): 315–338.

[22] Kennedy, R.C., and Short, S.A. (1994) "Basis for seismic provisions of DOE-STD-1020". United States. https://doi.org/10.2172/10146835

[23] FEMA (2018a). "*FEMA P-58-1, Sesimic Performance Assessment of Buildings, Volume 1 – Methodology*". Second Edition. Editors: AT Council, Federal Emergency Management Agency, Washington, D.C., USA. https://femap58.atcouncil.org/documents/fema-p-58/24-fema-p-58-volume-1-methodology-second-edition/file

[24] Abdullah, S.A., and Wallace, J.W. (2019) "Drift Capacity of RC Structural Walls with Special Boundary Elements" *ACI Struct. J*., **116**(1): 183–194.

[25] Eem, S., and Hahm, D. (2019) "Large strain nonlinear model of lead rubber bearings for beyond design basis earthquakes" *Nuclear Engineering and Technology*, **51**(2): 600–606.

[26] Hamaguchi, H., Wake, T., Yamamoto, M., and Kikuchi, M. (2019). "Practical application of lead rubber bearings with fail-safe mechanism" *Japan Arch. Rev*., **2**(3): 323–339.

[27] Muramatsu, Y., Inoue, K., Katoh, R., Kamitani, N., Sakaguchi, T., Sasaki, Y., Suzuki, S., Sera, S., Miyazaki, M., Kitamura, H. (2004). "Test results of ultimate properties of rubber bearings for building (Structures)," *AIJ Journal of Technology and Design*,**10**(20): 67–70.